



REPORT

Estimation of unrecorded groundwater abstractions in Jordan through regional groundwater modelling

M. Gropius¹ · M. Dahabiyeh² · M. Al Hyari³ · F. Brückner¹ · F. Lindenmaier¹ · S. Vassolo¹

Received: 28 October 2021 / Accepted: 19 July 2022 / Published online: 19 August 2022
© The Author(s) 2022

Abstract

Jordan suffers from water scarcity and groundwater covers the majority of Jordan's water supply. Therefore, there is an urgent need to manage this resource conscientiously. A regional numerical groundwater flow model, developed as part of a decision support system for the country of Jordan, allows for quantification of the overexploitation of groundwater resources and enables determination of the extent of unrecorded agricultural groundwater abstraction. Groundwater in Jordan is abstracted from three main aquifers partly separated by aquitards. With updated geological, structural, and hydrogeological data available in the country, a regional numerical groundwater flow model for the whole of Jordan and the southernmost part of Syria was developed using MODFLOW. It was first calibrated for a steady-state condition using data from the 1960s, when groundwater abstraction was negligible. After transient calibration using groundwater level measurements from all aquifers, model results reproduce the large groundwater-level declines experienced in the last decades, which have led to the drying out of numerous springs. They show a reversal of groundwater flow directions in some regions, due to over-abstraction, and demonstrate that documented abstractions are not sufficient to cause the observed groundwater-level decline. Only after considering irrigation water demand derived from remote sensing data, the model is able to simulate these declines. Illegal abstractions can be quantified and predictive scenarios show the potential impact of different management strategies on future groundwater resources.

Keywords Groundwater modelling · Jordan · Over-abstraction · Management scenarios

Introduction

Jordan is located in the Middle East (Fig. 1) and borders Israel, Saudi Arabia, Iraq, Syria and parts of Palestine. To the west, the Jordan Rift Valley includes the Dead Sea with an elevation of -420 m above sea level (a.s.l.), where the lowest accessible point on Earth is found. The eastern escarpment of the Jordan Valley rises to elevations of above 1,400 m a.s.l. and a Mediterranean climate prevails with significant rainfall of up to 600 mm/year in winter months and a dry and hot summer. To the east and southeast of the

escarpment, topography flattens significantly and climate rapidly changes to arid conditions.

Jordan is one of the nations with the highest water scarcity, defined as the annual renewable water resources per inhabitant below 300 m³. According to FAO-AQUASTAT, Jordan had in 2018 a value of 94 m³ per inhabitant per year. Surface water is only available in the western part of the country either in the high mountains, where precipitation is enough to produce runoff, or in the Jordan graben, where the Jordan River flows. Therefore, most water needs are supplied by groundwater, which presently meets 70% of the demand (Salameh 2008).

For the last 30 years, water demand has increased continuously in Jordan, due to population growth and a steady expansion of intensive agriculture. To cope with demand, groundwater exploitation was intensified and wells drilled to increasing depths. Today, aquifers are overexploited, leading to dramatic drawdown (MWI, BGR 2019), which threatens groundwater availability.

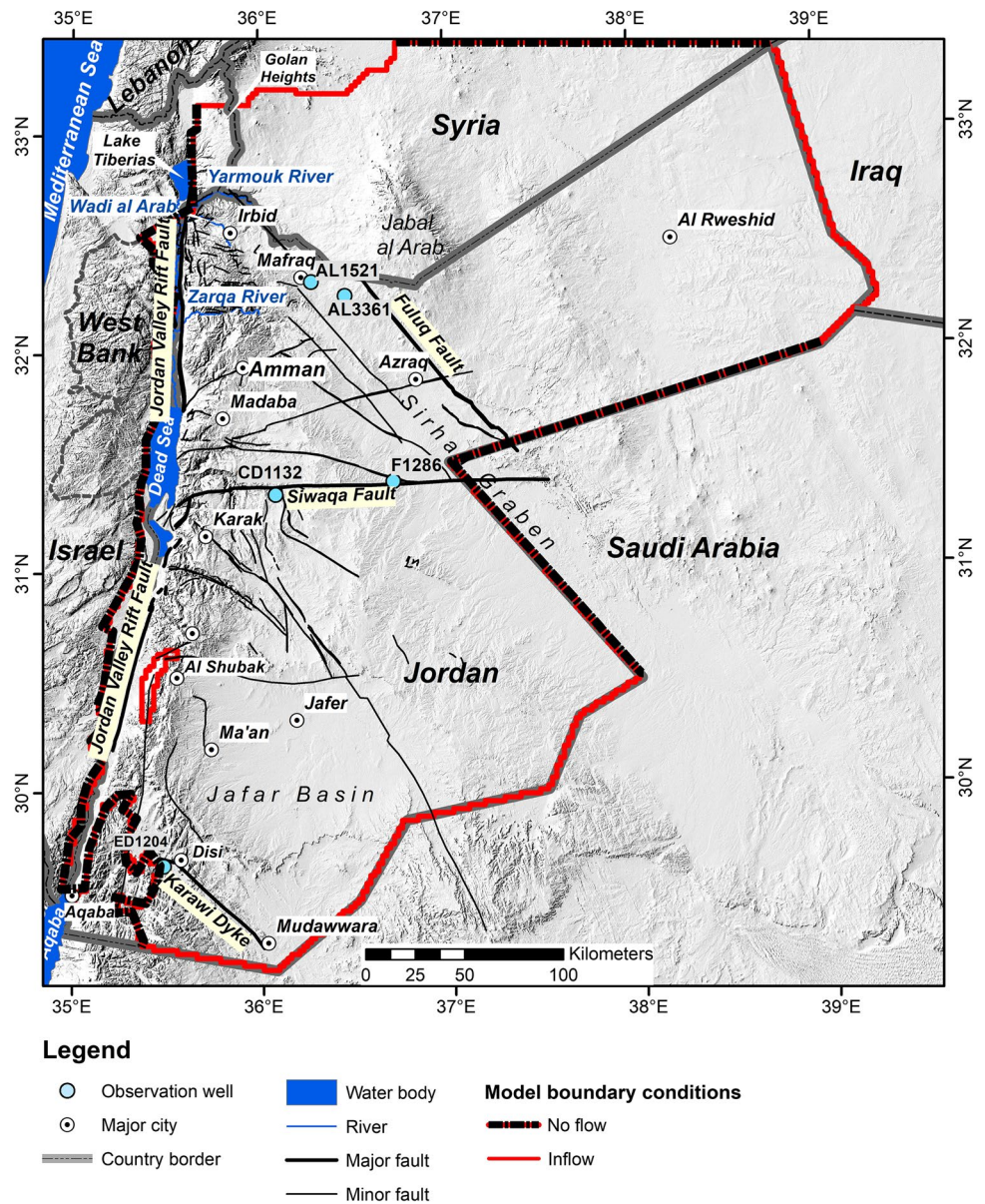
✉ S. Vassolo
saraines.vassolo@bgr.de

¹ Bundesanstalt für Geowissenschaften und Rohstoffe,
Stilleweg 2, 30655 Hannover, Germany

² Ministry of Water and Irrigation, Amman,
Hashemite Kingdom of Jordan

³ Groundwater Management Project, BGR, Amman,
Hashemite Kingdom of Jordan

Fig. 1 Geographical overview of Jordan with model boundary conditions, major structures, major cities, and observation wells used for calibration



A similar situation prevails in many other countries and regions in the world where arid climate conditions prevent increasing water demand from being met, due to population growth and extensive groundwater abstraction. Kalbus et al. (2011) identified agricultural water use as one of the most important components of the water budget for the upper Mega Aquifer System on the Arabian Peninsula. Gossel et al. (2004) studied the prehistorical groundwater development of the Nubian Sandstone aquifer in Eastern Sahara estimating groundwater origin and highlighting water balance deficits. Dodo (2011) developed a large-scale transboundary groundwater model for the Iullemeden aquifer system located in Mali, Niger and Nigeria aiming to investigate groundwater management options. Allani et al. (2019) and Nouiri (2021) coupled MODFLOW and WEAP models to

develop a decision support system (DSS) for a large watershed in Tunisia. Using remote sensing data, they were able to assess the unrecorded agricultural water use in order to improve the DSS.

In Jordan, groundwater modelling is commonly used for assessing the effects of aquifer exploitation and has a long tradition. Modelling studies date back to the late 1960s (FAO and UNDP 1968), early 1970s (FAO and UNDP 1972a, b), and late 1980s (Bender et al. 1989). The first nationwide groundwater model (Schmidt et al. 2008) was developed in the framework of the second Water Master Plan of Jordan (MWI 2005) and updated by Barthelemy et al. (2010); however, these studies include only parts of the aquifer system.

The Jordan Ministry of Water and Irrigation (MWI) already uses a water allocation model (WEAP) for water

management purposes. Since groundwater is the major source for water supply in Jordan and WEAP cannot reflect the complex hydrogeological and hydraulic processes, a new effort was undertaken to produce a flow model for the country (Fig. 1) that includes all relevant aquifers for coupling with the existing WEAP model. This report focusses on the numerical groundwater flow model. The model is based on geological and hydrogeological data as well as modelling results from previous regional studies (Hobler et al. 1991, “Groundwater resources of southern Jordan”, unpublished report; Mull and Holländer 2006; Barthelemy et al. 2007, 2010) and recent structural analyses (Brückner et al. 2021). This article describes the model construction as applied to Jordan, presents the most important results, and shows expected drawdowns under different management scenarios.

Materials and Methods

First, a hydrogeological concept model was produced based on an available three-dimensional (3D) geological model to finally develop the numerical groundwater model. This section also describes the boundary conditions adopted for the modelling as well as data used to feed them.

Conceptual model

Geological and hydrogeological units

The geological 3D model is based on a regional model compiled by BRGM (Barthelemy et al. 2010) that extends over Saudi Arabia, Jordan, and Syria. Data provided by BRGM concerns Jordan as well as south Syria and describes formations from Precambrian basement to Quaternary (Fig. 2).

According to the BGRM model (Fig. 2), the lowest *Ram group* (Cambrian to Ordovician) consists mainly of medium-to-coarse-grained siliciclastics that unconformably overlie the peneplained crystalline complex (Barthelemy et al. 2010; Powell et al. 2014). The sediments were deposited quickly and groundwater is discharged by a system of braided rivers in a coastal environment, which apparently extends over the whole of Jordan. Thickness increases towards the northeast reaching more than 2,000 m in the Wadi Sirhan depression (BGR/ESCWA 2013). Outcrops are found along the Dead Sea Rift escarpment and in the south. The Ram group is a major aquifer for Jordan. Groundwater inflows from Saudi Arabia in the south–southeast and flows towards the Dead Sea. Presently, recharge is negligible. It is assumed that groundwater originated in the last pluvial period some 5,000 BP.

The Silurian *Khreim group* is composed of five formations and overall considered as an aquitard (Fig. 2). The lowest Sahl as Suwaan Fm. consists of laminated

micaceous siltstone and fine-grained sandstone with abundant fluvial sedimentation features (cross lamination, ripples). Upward coarsening indicates high flow rates in the lower part of the formation, whereas a second shallow cycle led to an outer to mid-shelf depositional environment forming the first fully marine horizon with macrofossils (Powell 1989). Its equivalent in Saudi Arabia (Hanadir Shale) has a thickness of 54–100 m (Alsharhan et al. 2001). Outcrops of this formation have a thickness of approximately 30 m, but drilling results show maximum thicknesses of 189 m at Risha gas field (Margane and Hobler 1994). The formation builds an important aquitard covering the Ram group. The following Umm Tarifa Fm. consists predominately of micaceous fine-to-medium-grained sandstone and shows extensive bioturbation and was deposited in shallow water near a shore environment (Powell 1989). The overlying Trebeel Fm. is a predominantly sandy interval and represents the infill of incised glacial paleo-valleys (Barthelemy et al. 2010). These Umm Tarifa and Trebeel formations are aquifers that might be in contact with the overlying Kurnub sandstones. Hydraulic connectivity however is limited, due to their location between the Sahl as Suwaan and Alna/Batra aquitards (Barthelemy et al. 2010). The upper Alna and Batra Fms. are grouped together, because of their common lithology of alternating sandstone and siltstone deposited in a marine environment. The facies change from underlying glacial formations to shallow marine ice margin, indicating a transgressive event (Armstrong et al. 2009). Due to the intercalation of fine sediments, these formations act as an aquitard.

The *Zarqa group* was built over Permian, Triassic, and Jurassic. It comprises three different formations and as a whole is considered an aquifer (Fig. 2). The lowest Hudayb Fm. consists mainly of Permian sandstones that cover pre-Permian unconformity surfaces (Barthelemy et al. 2010) of the Ram group in the NW of Jordan and the Khreim group further east (Margane and Hobler 1994). The sediments show an upward fining sequence with conglomeratic sandstone at the bottom, fine-grained sandstone in the center, and siltstone/claystone at the top. The alluvial origin is indicated by ripples and cross-bedding (Bandel and Salameh 2013). From a hydrogeological point of view, this formation is a minor aquifer. The overlying Ramtha Fm. is composed of six members, which are distinguished based on lithology (sandstone, limestone, dolomite, shales, and gypsum). The Triassic environment of deposition varies from tidal to fully marine and reaches a total thickness of 1,000 m (Bandel and Salameh 2013). It crops out along the coast of the Dead Sea and is a major aquitard. The marine Jurassic carbonates of the covering Azab Fm. build a thick wedge of several thousand meters in the north of Jordan and Palestine. Sandstones, siltstones, and limestones were

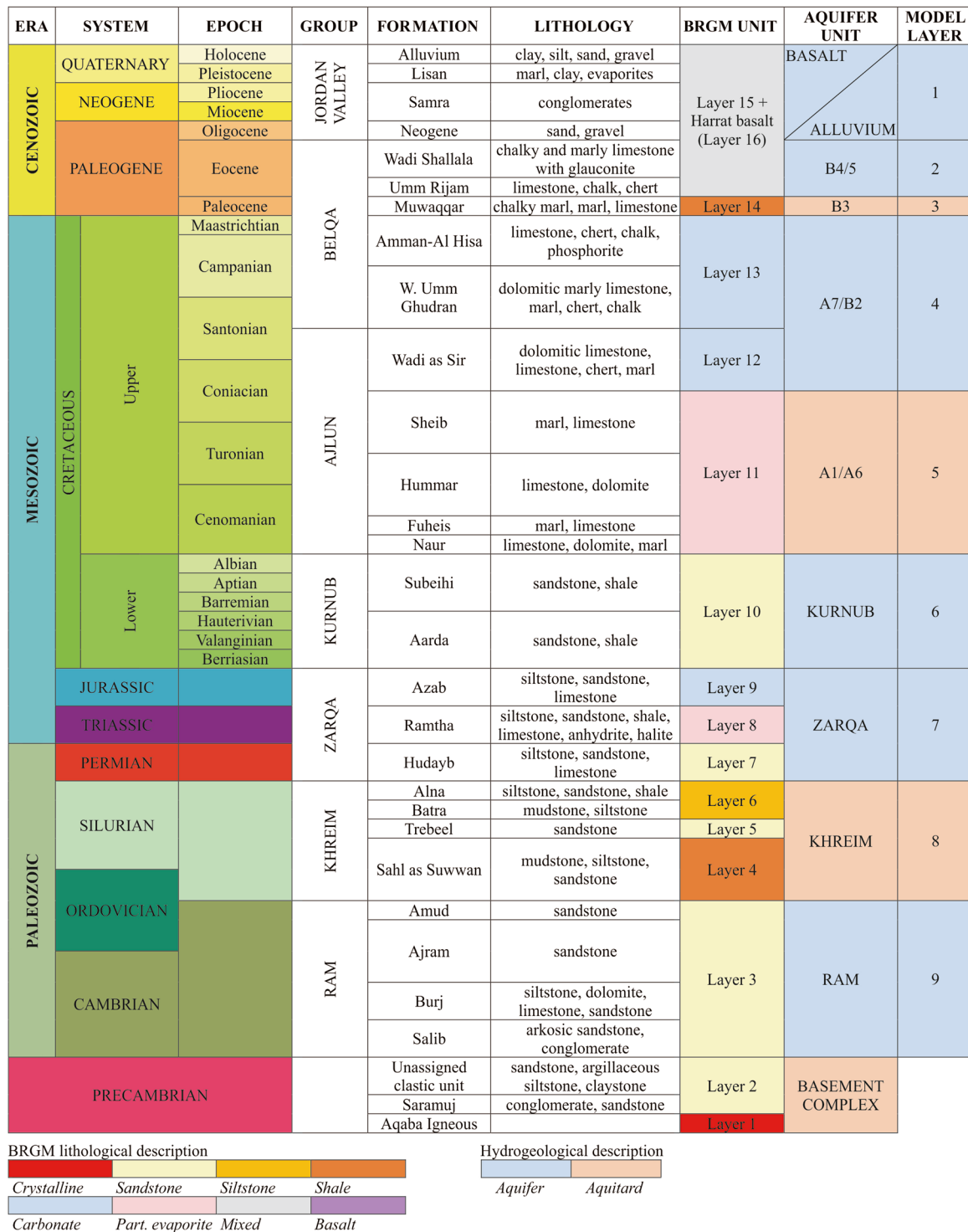


Fig. 2 Stratigraphy and hydrogeological grouping for Jordan (El-Naser 1991; Margane et al. 2002)

deposited on a subsiding shelf and show several circles of rising and falling sea levels (Bandel and Salameh 2013). They form a fractured aquifer (Barthelemy et al. 2010).

The *Kurnub group* is composed of sandstones that mark the base of a Lower Cretaceous transgression event (Fig. 2). It is hydraulically connected to the Ram aquifer in the western part of Jordan, but separated by the Khreim aquitard in the east. Thickness increases towards the north-east and reaches 30–150 m near Azraq (Barthelemy et al. 2010). Outcrops occur south of Zarqa River, in the lower slopes of the rift escarpment, and in deeply incised wadis. It is considered a major aquifer.

The *A1/A6 group* assembles the lower formations of the Upper Cretaceous Aljoun group and consists of marl, limestone, dolomite, and shale. The Naur (A1/A2) and Hummar (A4) formations are mainly composed of limestone sequences. Outcrops occur northwest of Amman, at the slopes of the rift escarpment, and in incised wadis. Regionally, this group is an aquitard, although the Naur and Hummar formations built significant local aquifers. In areas with strong karstification, the A1/A6 group is hydraulically connected to the overlying A7/B2 formation (Margane et al. 2002).

The lower members of the Upper Cretaceous Belqa group (W. Umm Ghudran and Amman-Al Hisa formations) and the uppermost member of the Ajloun group (Wadi as Sir), although differentiated by stratigraphy and structural characteristics (Barthelemy et al. 2010), constitute the *A7/B2 group* (Fig. 2). Outcrops form major parts of the Jordan highlands and underlie the whole country to the east. In the highlands, where the largest amount of precipitation takes place, recharge is enhanced by karstification, making the A7/B2 group the most important aquifer in Jordan. In the highest elevations, the aquifer is unconfined. Towards the east, where it is overlain by the B3 aquitard, groundwater occurs in confined conditions and artesianism occurs (Margane et al. 2002).

The Paleocene *Muwaqqar Fm.* (Fig. 2) consists of chalky to marly limestones and cherts that were deposited in a shallow shelf environment. Most of the proven oil shale reserves in Jordan are encountered in the lower part of this formation, due to locally elevated contents of bitumen (Ziegler 2001). This formation is known as B3 in Jordan and acts as an aquitard.

The BGRM model groups all upper Paleogene, Neogene, and Quaternary formations as “top formation” (Barthelemy et al. 2010). Because the aim of the groundwater model was to evaluate the behaviour of all relevant aquifers in Jordan, the younger units (B4/B5, the Jordan Valley Fm., and the Harrat basalt) had to be differentiated. For this activity, published information was incorporated (Margane and Zuhdi 1995; Margane and Almomany 1995; Schmidt et al. 2008).

The *B4/B5 group* includes the Eocene Umm Rijam (B4) and Wadi Shallala (B5) formations as well as the alluvial Dead Sea rift filling (Fig. 2) and consists of chalk, chalky marl, and chalky limestone with intercalations of limestone and chert nodules (Margane et al. 2002). It does not occur in the Jordanian highlands and southern Jordan. Apart from the Wadi Sirhan graben, the thickness of the two formations is relatively low. The group forms shallow aquifers recharged by wadi baseflow, floods, precipitation, and irrigation return flow. The depth to water table varies widely from around 150 m along the escarpment foothills to only 5 m in the central valley (USGS 1998).

The *Jordan Valley group* consists of soil, sand, and gravel deposited along the Jordan graben as well as alluvial fans along both sides of the escarpment. The group is an aquifer.

The Tertiary to Quaternary *Harrat basalt* is the Jordanian part of the North Arabic Volcanic Province that includes the Golan Heights as well as the Harrat Province in Saudi Arabia and is centered on the Jebel al Arab in southern Syria. The province consists of Neocene plateau basalts, Quaternary lava flows, and shield volcanoes (Wagner 2011). The thickness of individual lava flows vary from 3 to 25 m. The total thickness of the basalt reaches 1,500 m at the Jebel Al Arab and diminishes radially. In Jordan, the maximum value is around 500 m (Margane et al. 2002). The top of the Jebel al Arab Mountain is the main recharge area for this fractured aquifer. Groundwater flow follows roughly the topographic gradient away from the mountain and is highly anisotropic, with much higher horizontal conductivities between individual lava flows (BGR/ESCWA 1996). Many local perched aquifers occur between lava flows. Recharge of underlying formations occurs through faults and cooling cracks that enhance downward leakage. In Jordan, the basalt is partly connected to the B4/5 aquifer, the B3 aquitard, and the A7/B2 aquifer.

The groundwater model also considers the most important tectonic structures described by Bender (1974) and (1975), and Hobler et al. (1994) for Jordan, especially those with significant offsets throughout the model domain (Fig. 1). The Jordan Valley fault system, the Fuluq Fault, which delimits the Sirhan depression to the east and gives place to vertical displacements of more than 2,000 m (Hobler et al. 1994), and the basaltic Karawi dyke, which extends from Mudawara northwestwards to the Jordan Valley escarpment and acts as a hydraulic barrier, were incorporated.

Summarizing, the hydrogeological system of Jordan consists of three major aquifer systems separated by aquitards (Margane and Saffarini 1994). Alluvial sediments in the Dead Sea rift basin as well as the Neogene basalt flow of the Jebel al Arab Volcano in Syria and the underlying B4/5 formations define the shallowest aquifer system. The middle aquifer system A7/B2 constitutes the most important source of water supply in Jordan. In general, the B3

Table 1 Lateral boundary conditions along the model borders

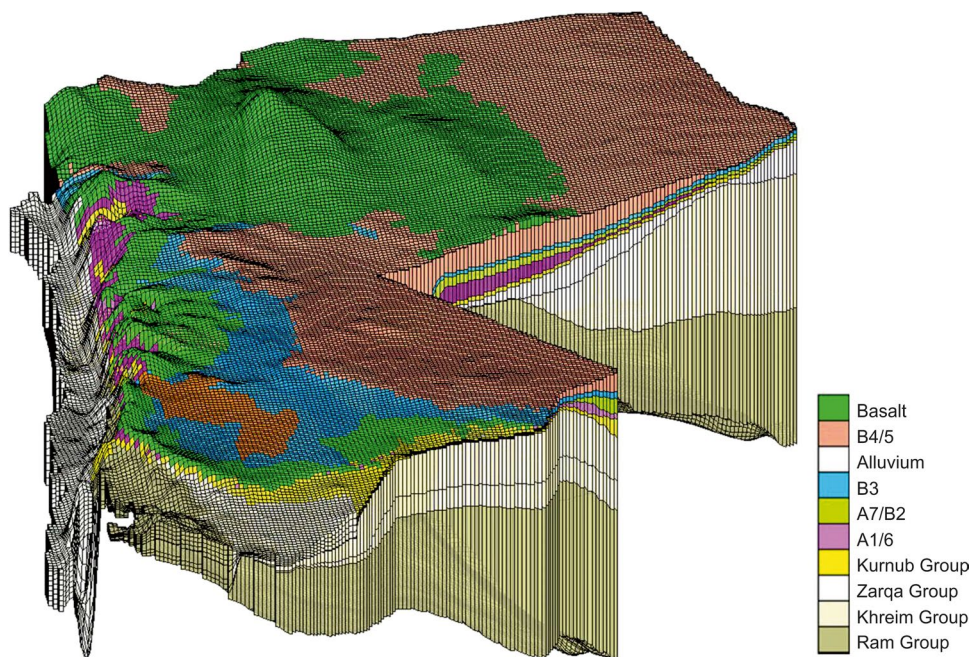
Border	Hydrogeological unit	Type (steady state)	Type (transient)
Southern border to Saudi Arabia	Ram	Constant head, 935 m a.s.l. (W) to 585 m a.s.l. (E)	Fixed flux (wells)
Eastern border to Iraq/Saudi Arabia	A7/B2	No flow, if existent	No flow, if existent
	Ram	Constant head	Fixed flux (wells)
Northwestern border	A7/B2	None, A7/B2 unsaturated	None, A7/B2 unsaturated
	B4/5	Constant head –265 m a.s.l.	Fixed flux (wells)
Jordan River	Alluvium	Constant head from –265 m to –395 m a.s.l.	Constant head (steady state)
Dead Sea	Alluvium	Constant head –395 m a.s.l.	Transient head –395 m a.s.l. (1960) to –429 m a.s.l. (2014), declining 1 m/year afterwards
Red Sea	Alluvium	Constant head 0 m a.s.l.	Constant head 0 m a.s.l.

formation separates both aquifer systems except in northern Jordan, where the basalt aquifer overlies directly the A7/B2 (Margane et al. 2002). The deepest aquifer system is composed of several sandstone aquifers of Cambrian (Ram aquifer) to Lower Cretaceous age (Kurnub aquifer) (Fig. 2). Subformations of the Ajloun group (A1/A6) and the whole Khreim group are aquitards that separate the middle from the deeper aquifer systems and the Kurnub from the Ram aquifer, respectively (Fig. 2). The bottom of the model is defined by the Precambrian basement. Hydraulic connections between different aquifers might occur locally, as is the case of the Ram and Kurnub aquifers in southwestern Jordan, due to the absence of the Khreim aquitard (Margane et al. 2002).

Boundary conditions

Lateral, along the model borders Groundwater in- and out-flows at the boundaries follow the conceptual hydrogeological model (Table 1). For the steady-state model, constant head boundary conditions are applied following published values (Barthelemy et al. 2010). The steady-state flux calculated at each constant head node was then used as a fixed flux boundary for the transient flow modelling. The western boundary is assigned as ‘no flow’, since no groundwater flows to or from the west.

Springs and Azraq wetlands There are 861 reported springs in Jordan (MWI 2018), the majority are located at

Fig. 3 Three-dimensional view of the groundwater 3D model

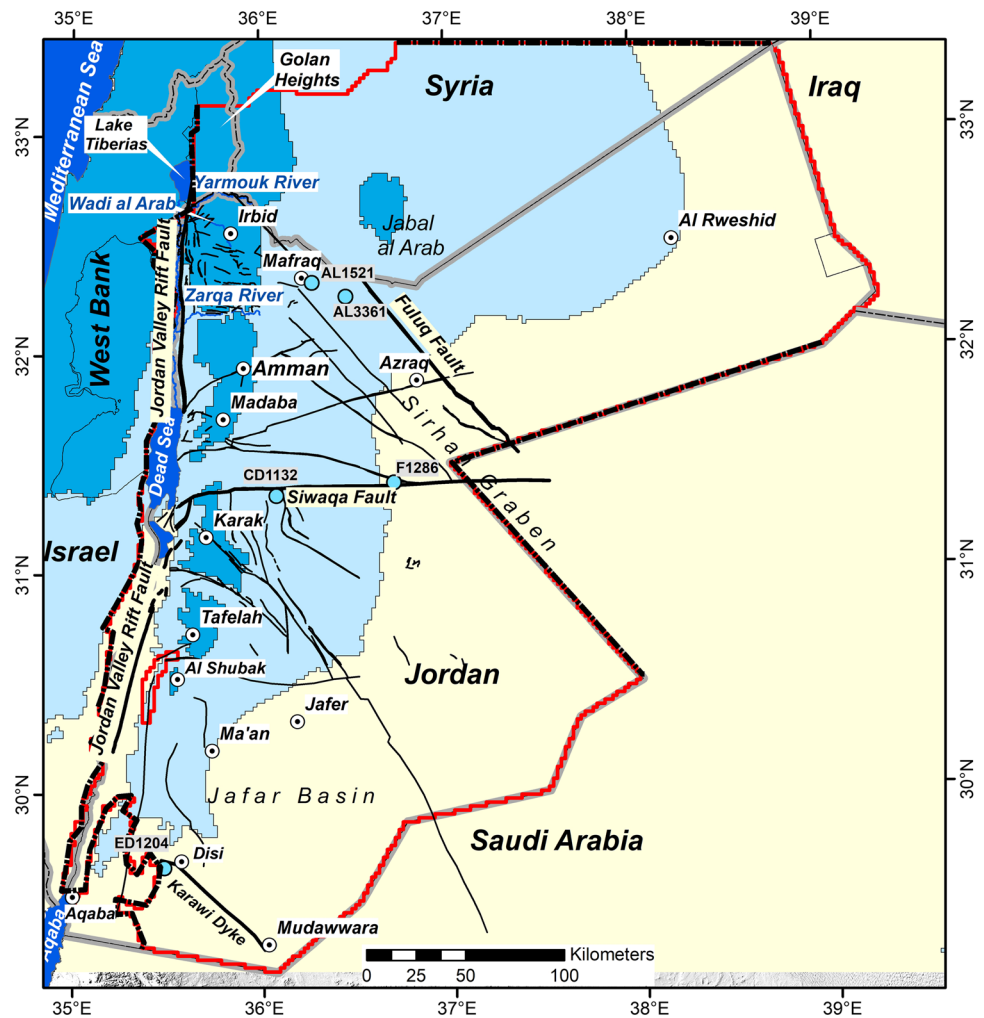
the escarpment of the eastern Jordan Valley bank and its steep sided wadis. The model considers 49 springs with discharge larger than 150 m³/h and locally well-known springs with drain boundary conditions. Outflow elevations were obtained either from the BGR geodetic survey (MWI, BGR 2019), the MWI database, or Google Earth. The Azraq wetlands are located in a topographic depression and used to be flooded with spring water and ascending groundwater. The two springs annually discharged 14 million cubic meters (MCM) in 1963/1964 (Margane and Zuhdi 1995). Groundwater-irrigated agricultural development and the start of a municipal wellfield operation in 1982 caused a continuous decline in groundwater levels that led to the drying out of the springs in 1993. The two springs, with an outflow elevation of 515 m a.s.l., were represented in the model with a drain boundary condition. Further drain boundary conditions

were applied to seven cells within the area of the wetland at 508 m a.s.l. to reflect groundwater seepage at the bottom of the depression at historic times.

Wadis/rivers Because generally rivers are ephemeral, discharge from side wadis of the Jordan Valley and the Yarmouk River were assigned as drain boundary conditions. Riverbed elevations were estimated based on the SRTM elevation data and Google Earth. The Jordan River was defined as constant head (Table 1) for simplification. A general lack of water level data and only minor water level fluctuations justify this approach.

The *Dead Sea* was assumed as constant head at −395 m a.s.l. in the steady-state model. Time-dependent heads varying from −395 m a.s.l. in 1960 to −429 m a.s.l. in 2014 were used in the transient model. The Dead Sea

Fig. 4 Precipitation and groundwater recharge distribution adopted for the steady-state conditions



Legend

- Observation well
- ⊙ Major city
- Country border
- Major fault
- Minor fault
- Water body
- River
- Major fault
- Minor fault
- Model boundary conditions**
- No flow
- Inflow
- Precipitation / Recharge**
- < 75 mm / no recharge
- > 75 mm / 2.5 mm
- > 300 mm / 10 mm

Table 2 Range of hydraulic properties obtained by calibration for all hydrogeological units in the model

Hydrogeological unit	K_h [m/s]	K_v [m/s]	Spec. storage [1/m]	Spec. yield [–]	Porosity [%]
Basalt	1.0×10^{-4}	1.0×10^{-04}	1.0×10^{-7}	0.05	5%
B4/5	8.0×10^{-5}	$8.0 \times 10^{-6} - 8.0 \times 10^{-5}$	$1.0 \times 10^{-7} - 1.0 \times 10^{-5}$	0.03–0.10	2–5%
Alluvium (Jordan Valley)	$1.0 \times 10^{-5} - 1.0 \times 10^{-4}$	$1.0 \times 10^{-5} - 1.0 \times 10^{-4}$	1.0×10^{-6}	0.10	10–15%
B3	$1.0 \times 10^{-7} - 2.0 \times 10^{-7}$	$5.0 \times 10^{-9} - 1.0 \times 10^{-8}$	1.0×10^{-6}	0.001	0.1–1.0%
A7/B2	$1.0 \times 10^{-5} - 2.0 \times 10^{-4}$	$1.0 \times 10^{-7} - 2.0 \times 10^{-5}$	$1.0 \times 10^{-6} - 1.0 \times 10^{-5}$	0.025–0.10	4%
A1/6	$2.5 \times 10^{-6} - 5.0 \times 10^{-7}$	$2.5 \times 10^{-8} - 2.0 \times 10^{-11}$	1.0×10^{-6}	0.01–0.04	2%
Kurnub	5.0×10^{-6}	5.0×10^{-7}	1.0×10^{-6}	0.025	2%
Zarqa Group	2.5×10^{-6}	2.5×10^{-8}	7.0×10^{-7}	0.01	1%
Khreim Group	5.0×10^{-7}	5.0×10^{-9}	7.0×10^{-7}	0.01	1%
Ram	$1.8 \times 10^{-5} - 2.5 \times 10^{-5}$	$1.8 \times 10^{-5} - 2.5 \times 10^{-5}$	7.0×10^{-7}	0.05–0.10	2–10%

K_h horizontal hydraulic conductivity; K_v vertical hydraulic conductivity

receives most of the unused Jordanian groundwater. Nevertheless, its water level declines about 1 m/year due to high evaporation and reduced inflow of Jordan River water.

Wells According to the MWI database, 3,272 wells were operating in 2017 (MWI 2018). In MODFLOW, wells are assigned to cells according to their location. If several wells are located in the same model cell, the individual abstraction rates are summed up for the respective cell; thus, an assessment of hydraulic heads at individual wells is impossible. The aquifer from which groundwater is abstracted is generally included in the database. Where no data are available, the pumped aquifer is estimated based on information from well depth and layer depth, as it is assumed that the screened section is always at the bottom of the well. Wells are exclusively assigned to one layer in the model.

Horizontal flow barrier (HFB) This type of boundary is applied for the Jordan Valley fault, Siwaqa fault (only Ram to A1/A6) and the Karawi dyke. The permeabilities of the horizontal flow barriers (HFB) were estimated during the calibration process, taking into account the measured hydraulic heads on both sides of the faults, and are generally lower than aquifer properties. The Fuluq Fault that delineates the Sirhan depression is represented by changes in layer elevations and is therefore nonvertical.

Numerical model

The groundwater flow model was implemented in MODFLOW-2005 (Harbaugh 2005) using the Newton-Raphson formulation (MODFLOW-NWT; Niswonger et al. 2011) and covers an area of 109,564 km² resulting in a horizontal grid with 27,391 active cells with a size of 2,000 m × 2,000 m. No local grid refinements were made because the subsequent

coupling with WEAP requires a regular grid size. Due to political restrictions and lack of data, the model area is limited by the border to Saudi Arabia in the south and southeast (Fig. 1). The limit to the Iraq border is explained by the fact that no recharge occurs in Iraq and groundwater levels at the border are reported to lay below the base of A7/B2; thus, no inflow from or outflow to the east can be expected for the upper and middle aquifers. To the north, the model extends into Syria to include the area of Jebel al Arab Mountain, which is the recharge zone for the basalt aquifer. The western bank of the Jordan Valley limits the model area to the west.

Vertically, the model is subdivided into nine layers to include each of the previously defined units (Fig. 2), resulting in a 3D grid with 246,519 active cells (Fig. 3). Layer elevations were derived from the BRGM structural model (Barthelemy et al. 2010), but needed to be smoothed along the eastern bank of the Jordan Valley and the Fuluq Fault to avoid numerical instabilities. Ground surface elevations were derived from SRTM data (NASA 2020) and vary from

Table 3 Number of monitoring points used for model calibration

Hydrogeological unit	Model layer	Steady state	Transient
Alluvium (Jordan Valley)	1	10	2
Basalt	1	2	2
B4/5	2	6	12
B3	3	–	–
A7/B2	4	42	21
A1/6	5	–	6
Kurnub	6	–	1
Zarqa Group	7	–	2
Khreim Group	8	–	–
Ram	9	22	9
Total	–	82	55

1,803 m a.s.l. in the highlands to -750 m a.s.l. in the lowest point of the Dead Sea floor. The ground surface elevation partly deviates from SRTM data, where significant topography changes occur over small distances, due to the model grid size. This is the case, especially along the eastern escarpment of the Jordan Valley and its steep side wadis. At the bottom of the model, elevations vary between 1,500 and $-6,500$ m a.s.l. Model layers have variable thicknesses and layer elevations show significant incline at fault locations. Hydraulic conditions vary between phreatic, confined and even artesian (Ram aquifer in Disi area and B4/5 in Azraq area).

Data

Precipitation and groundwater recharge

Precipitation distribution was based on the WorldClim Version 1.4 (release 3) data set (Hijmans et al. 2005). The highest long-term mean annual rainfall occurs in the highlands of Jordan (540 mm) and in Syria (975 mm), while less than 75 mm fell in the southeast and the Wadi Araba (southern Jordan Valley). The long-term mean annual precipitation for the model area sums up to 11,286 MCM.

According to Margane et al. (2002), various water balance models estimate the overall groundwater recharge in Jordan at 280 MCM/year nowadays, which is about 3.3% of the total annual precipitation.

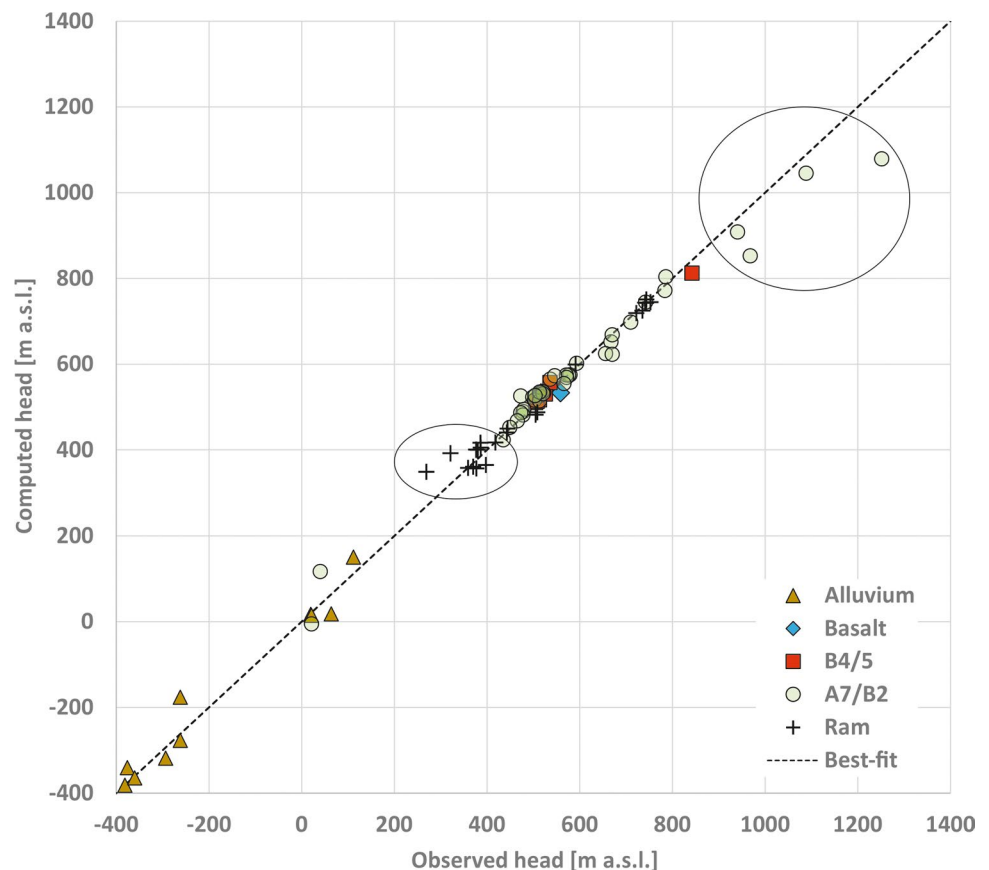
Recharge distribution correlates with precipitation distribution and the amount depends on the type of outcropping rocks. In the model, higher recharge values were set at the karstified outcropping limestone (A7/B2), whereas no recharge was considered at the outcropping of B3 formation, which is almost impermeable (Fig. 4). Highest recharge occurs in the highlands and on the Jebel al Arab Mountain in southern Syria, where the basalt aquifer is recharged. In areas with precipitation of less than 75 mm/year, recharge was neglected.

Transient annual groundwater recharge was varied following the deviation of the mean annual precipitation from the long-term mean annual precipitation (1960–1989) for each of the modelled years (1960–2017).

Groundwater levels from monitoring wells

Data from about 5,160 historic and actual wells are included in the database from which some 200 are used as monitoring wells. The database provides groundwater level data for them with heterogeneous quality concerning sampling rate,

Fig. 5 Calculated hydraulic heads vs. observed average groundwater levels



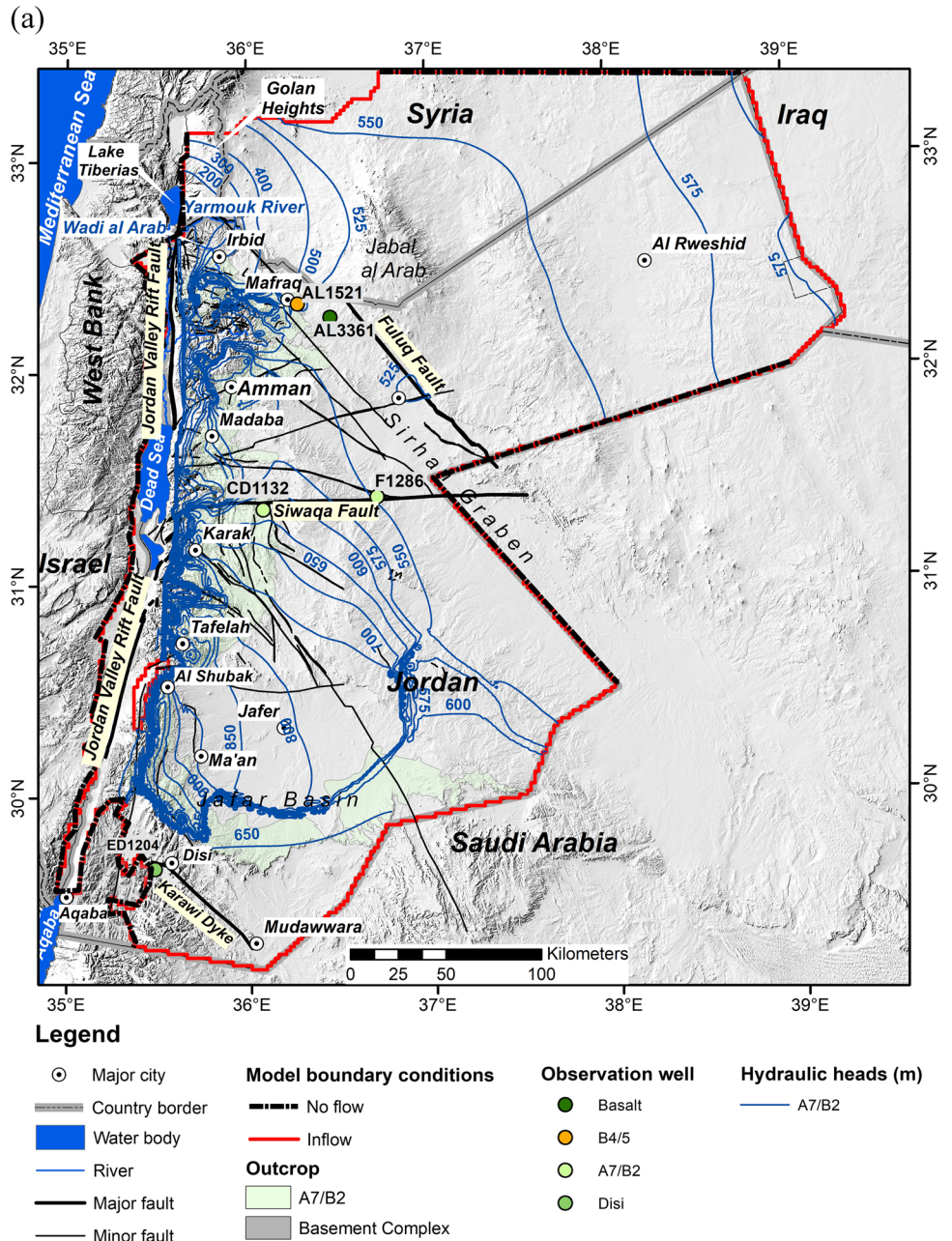
data gaps, length and data quality. An inventory (MWI, BGR 2019) showed that in 2017 only 80 monitoring wells were still delivering reliable data. These time series were used to verify the transient model against historical data.

Aquifer parameters

Estimated aquifer parameters are very sparse in Jordan. Parameter distributions for the individual model layers are not available, except for a limited area of the Disi aquifer in southern Jordan, where hydraulic parameters from

several reliable hydraulic tests are available. Initial values for horizontal and vertical hydraulic conductivities, specific yields, and porosity/specific storage for each of the modelled units (aquifer and aquitard) were taken from previous models (Schmidt et al. 2008; Barthelemy et al. 2010) and from the literature (Margane et al. 2002). In general, uniform parameter distribution applies to each layer. Hydraulic conductivities and storage coefficients reflect the type of layer according to the conception hydrogeological model. Higher conductivity values between 1×10 to 2×10^{-4} m/s with vertical anisotropy from 1 to 10 are assigned to the

Fig. 6 Simulated hydraulic head contour maps for pre-development status in aquifers **a** A7/B2 and **b** Ram. Black crosses indicate monitoring well locations



aquifer units, while values of less than 2.5×10^{-6} m/s and vertical anisotropy from 10 to 1000 are assigned to aquitard units (Table 2).

Pumping wells

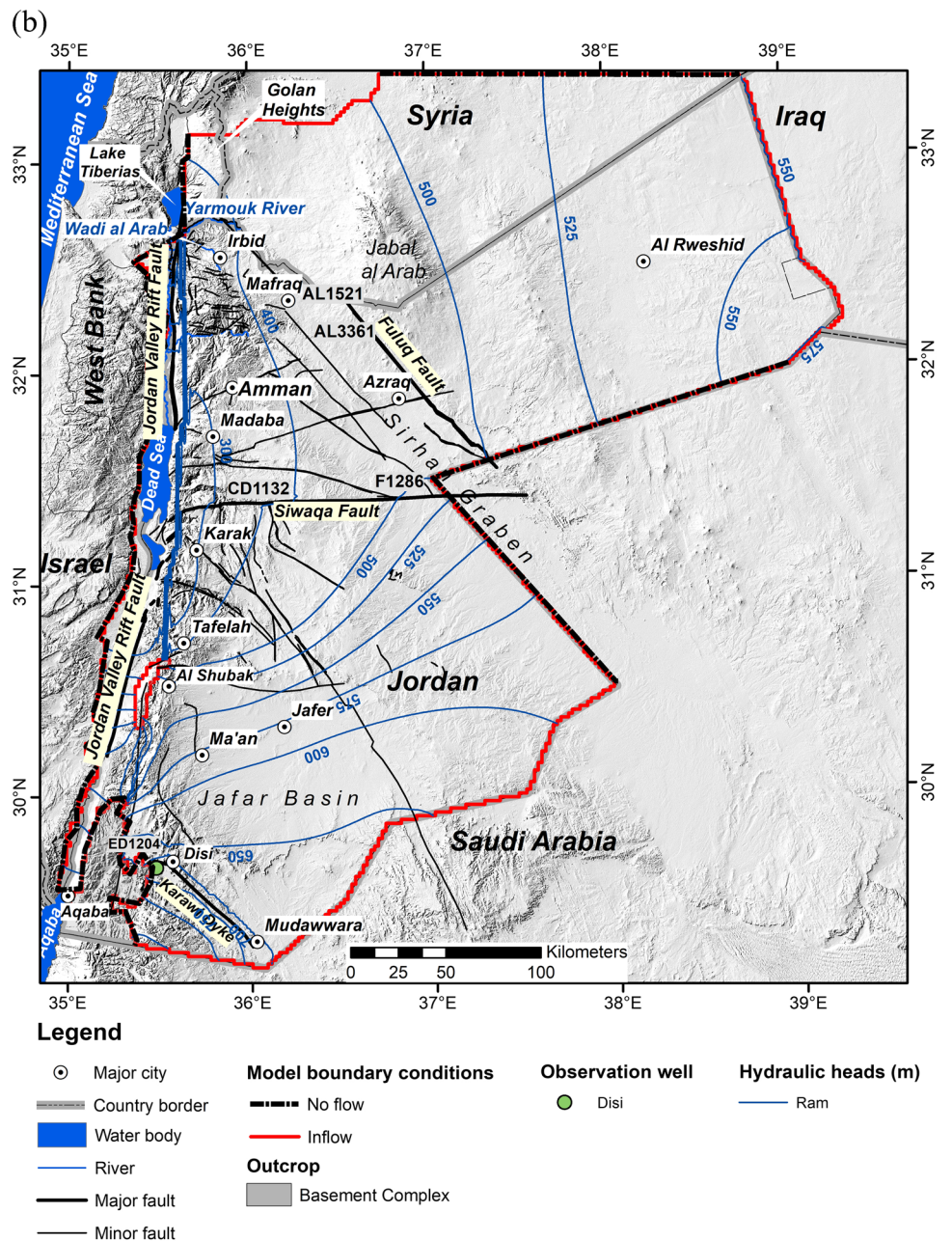
Abstraction rates and information on the type of use (domestic, industrial, irrigation) were obtained from the database at MWI.

For irrigation wells, the first recorded operation data do not coincide with the beginning of irrigated agriculture. To overcome this bias, the pumping rates were linearly extrapolated to zero at the time when agriculture

development reportedly started in the specific area. This approximation is more appropriate than neglecting the initial period of pumping activities. Nevertheless, significant uncertainties concerning groundwater abstraction remain, mainly due to illegal wells, unlicensed deepening, wells relocation, or broken flow meters. Recent studies using remote sensing data (Al-Bakri 2016) reveal discrepancies between the metered and documented abstractions for private and irrigation wells. The study concludes that real abstraction rates are 2.5–3 times higher than official values.

No pumping is considered outside Jordan, due to a lack of data.

Fig. 6 (continued)



Results and discussion

Steady-state calibration

The model was calibrated towards average water levels measured in the period 1960–1990 in 82 monitoring wells (Table 3), irrespective of the available number of entries for each individual well. These average values are considered to represent groundwater levels prior to the extensive agricultural development and the related increasing groundwater exploitation that started in the mid to late 1980s.

Table 2 lists the hydraulic properties obtained for each modelled unit after steady-state calibration. Due to the given data situation, the regional size of the model, and the coarseness of the grid, it was refrained from local parameter fitting, which would result in a detailed parameter distribution and potentially better fitting calibration, but not necessarily represent the reality. Only in wider areas, hydraulic conductivity values were altered to achieve a better fit of the calculated hydraulic heads. For A7/B2, the horizontal hydraulic conductivity of 1.0×10^{-5} m/s obtained with steady-state calibration needed alteration in the transient calculation. It required a reduction to 1.0×10^{-6} m/s in the recharge area south of Al-Shubak and an increase to 2.0×10^{-4} m/s in the Jafer basin to achieve a better fit the measured hydraulic heads.

In general, the calculated hydraulic heads correlate with the average groundwater levels used for the calibration, although some outliers appear at elevations from -250 to $+350$ m a.s.l. and above $+950$ m a.s.l. (Fig. 5). The first range corresponds to the steep escarpment of the eastern bank of the Jordan Valley, where model resolution does not allow a proper representation of the complex fault structure. The latter refers to an area in the highlands south of

Ma'an, where the hydrogeological setting is not yet fully understood. The average error (observed head minus calculated head) for all observation points is -1.55 m and the root mean square error (RMS-error) is 34.53 m. This error is approximately 2% of the overall hydraulic head range in the model domain (average heads used for the calibration range from -400 to 1300 m a.s.l.). Given the regional nature of the model, the grid size, and the fact that average groundwater levels from a large time period were used for calibration, the RMS error is suitable.

Modelled hydraulic heads and flow directions are in good accordance with published results (Barthelemy et al. 2010; MWI 2005). Calculated heads are able to represent the different flow directions in A7/B2 and Ram aquifers as well as the hydraulic head difference of several hundred meters between both aquifer systems (Fig. 6).

The total model inflow is 797.47 MCM and the total outflow 797.51 MCM with an imbalance of -0.04 MCM or 0.4%, which is acceptable for the size of the model. Most of the inflow is lateral from Saudi Arabia (269 MCM) through the Ram aquifer followed by groundwater recharge (260 MCM; Table 4). The highest discharge takes place into the Dead Sea (216 MCM) followed by discharge into the Yarmouk River (120 MCM). A significant outflow of 82 MCM from Jordan to Saudi Arabia occurs, where the Karawi dyke crosses the model boundary.

Transient simulation

The transient model simulates the period 1960–2017 using annual stress periods subdivided in 12 uniform time steps. The transient input data comprised water level of the Dead Sea, groundwater recharge, and pumping rates of abstraction wells, which are generally available as annual average

Table 4 Water budget analysis for steady-state conditions (MCM = million cubic meters)

Component	Inflow [MCM]	Outflow [MCM]	Literature [MCM]	Source
Inflow from the south (Ram)	269	82	300 (inflow)	MWI 2005; Mull and Holländer 2006
Inflow from the east (Kurnub - Ram)	78	43.5	90 (inflow)	MWI 2005
Outflow Azraq Oasis/wetland	–	19.9	12–18	Margane and Zuhdi 1995
Wadi Zarqa River	–	15.2	60	Margane et al. 2002
Wadi Kafrein and Shuayb	–	33	28	
Wadi Mujib	–	53	57	
Wadi Hasa	–	8.5	25.5	
Yarmouk river	–	122	120	
Outflow Dead Sea	–	216	210 300	MWI 2005; Mull and Holländer 2006
Inflow from North (Jebel Sheikh)	79	–	114	Estimation
Recharge	260	–	280	Margane et al. 2002
Pumping wells	–	23.5	–	Active wells in 1960

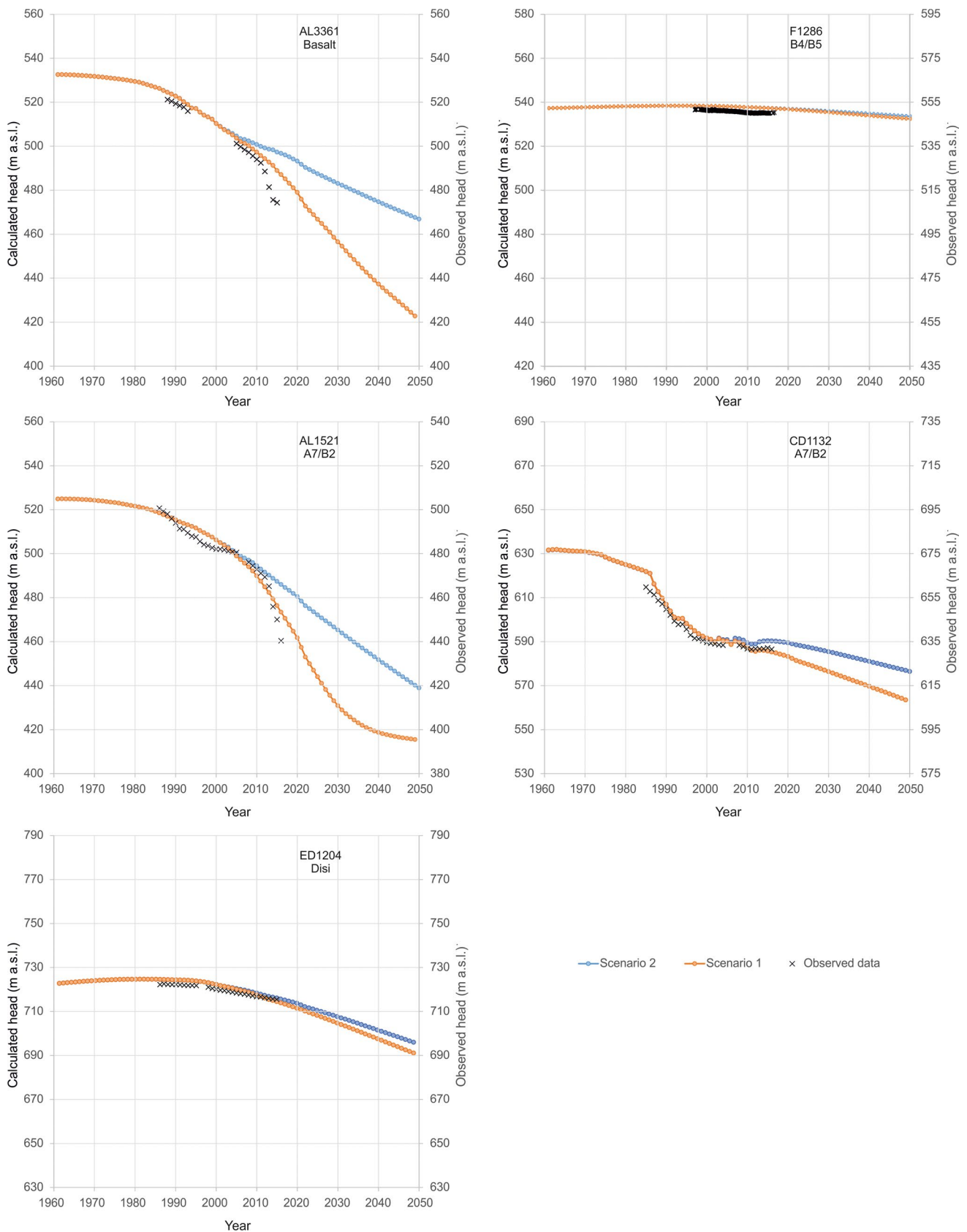


Fig. 7 Simulated and observed hydraulic heads for selected monitoring wells associated with the aquifer systems considered in the model (Basalt, B4/5, A7/B2, and Disi) for both scenarios (orange for scenario 1 and blue for scenario 2)

abstraction rates in the database. Annual groundwater recharge varies following the deviation of the mean annual precipitation from the long-term mean annual precipitation. Modelled steady-state groundwater heads represent the initial heads for the transient modelling. Groundwater level time series obtained from 55 monitoring wells were used for model calibration (Table 3).

Comparison of modelled and observed groundwater levels for selected monitoring points in different aquifer units (Fig. 6) illustrates the heterogeneity of the transient behavior regarding location and aquifer unit. Observed groundwater levels at well AL3361 in the basalt aquifer shows a decline of around 30 m for the period 1988–2012. Then the decline increases significantly with additional 20 m in the next 3 years (Fig. 7). The modelled hydraulic heads match the observed decline up to 2006, but fails to reproduce the later strong decline.

The model adequately replicates the small drawdown of 2 m measured in the B4/5 aquifer from 1995 to 2015 at monitoring well F1286, located approximately 50 km to the south of Azraq (Fig. 7). Most of the observed data correspond to the A7/B2 aquifer system, which is the most used in Jordan. Similar to AL3361 in the basalt aquifer, heads at well AL1521 show a significant drawdown increase after 2013, which is again not reproducible by the model. However, the calculated hydraulic heads at monitoring well CD1132 match the observed trends and absolute decline over the full simulation period (Fig. 7).

Calculated hydraulic heads reproduce the observed trends recorded at well ED1204 in the Disi aquifer (Fig. 7), although the calculated trend is slightly higher (3 m at the end of the modelled period).

The water balance at the end of the calculation period indicates a total inflow of 1754 MCM and a total outflow of 1,783 MCM with a difference of -28 MCM or 1.6%. The largest inflows (Table 5) are lateral inflow from Saudi Arabia through the Ram aquifer (266 MCM) and total groundwater recharge (267 MCM). Discharge to the Zarqa River has ceased, which reflects reality, since nowadays the river carries only treated wastewater from a large wastewater treatment plant.

The largest outflow corresponds to abstraction from wells (653 MCM) followed by discharges into the Dead Sea (601 MCM) and the Yarmouk River (120 MCM). The discharge to the Dead Sea has increased significantly compared to steady-state results, due to the continuous decline of sea-water table.

Table 5 Detailed water budget analysis for 2017 (MCM=million cubic meter)

Component	Inflow [MCM]	Outflow [MCM]
Inflow from the south (Ram)	266	69
Inflow from the east (Kurnub - Ram)	77	–
Wadi Zarqa River	–	0
Wadi Kafrein and Shuayb		1
Wadi Mujib		20.5
Wadi Hasa		5
Yarmouk River		120
Outflow Dead Sea	–	601
Springs	–	3
Recharge Jordan	267	–
Pumping wells (WIS)	–	653

Predictive modelling

The sudden decline in groundwater levels since 2010 is measured particularly in areas with intensive agricultural use. Because transient modelling using recorded abstractions for irrigation purposes is not able to reproduce the measured heads for the period 2010–2017 (Fig. 7), an alternative method for estimating irrigation abstractions was adopted. Based on Landsat 7 and Landsat 8 remote sensing data for 2014 and the derived normalized difference vegetation index (NDVI), Al-Bakri (2016) mapped the irrigated crops. Crop water requirements in the form of evapotranspiration (ET_c) were calculated following the FAO56 method (Allen et al. 1998). These values were adopted as pumped water for irrigation.

For evaluating future groundwater development, the model was run up to 2050. Pumping rates for industrial and domestic uses remained constant at 2017 levels for the whole calculated period, but two different pumping rates for irrigation were considered. In scenario 1, abstraction for irrigation was based on calculated crop demand for 2013 (Al-Bakri 2016), whereas scenario 2 considered irrigation abstraction rates as documented in the database for 2017 (Table 6). An annual groundwater demand for irrigation of about 450 MCM was adopted in scenario 1, which exceeds the documented abstraction used in scenario 2 by almost 75%.

Calculated heads at well AL3361 in the basalt aquifer and well AL1521 in the A7/B2 aquifer (Fig. 7) show a much better fit under scenario 1 than under scenario 2, especially for the last observed heads.

Table 6 Comparison of annual irrigation water demand according to respective sources (MCM = million cubic meter)

Agricultural areas	Scenario 1	Scenario 2	Difference [MCM]
	Data from crop needs [MCM]	Data from database [MCM]	
Mafraq agriculture	103.7	60.8	42.9
Zarqa agriculture	33.5	9.1	24.4
Zarqa agriculture (Azraq)	33.5	25.8	7.7
Ajloun agriculture	5.4	0.7	4.7
Amman agriculture	120.8	68.5	52.3
Irbid agriculture	17.6	3.2	14.4
Jerash agriculture	2.9	2.2	0.7
Karak agriculture	23.7	7.7	16.0
Maan agriculture	63.6	49.2	14.4
Madaba agriculture	6.3	2.9	3.4
Tafilah agriculture	5.1	3.2	1.9
Aqaba agriculture	32.4	23.6	8.8
Total	448.5	256.9	191.6

Irrespective of the irrigation abstraction scenario under consideration, drawdown of up to 100 m is predicted in Wadi al Arab area for 2050, which is produced by a major well-field that provides water to Amman (Fig. 8). As expected, the situation is worse for scenario 1, especially in central Jordan, where drawdown of 75 m is calculated.

Conclusion

A regional numerical groundwater flow model has been set up for Jordan. Because of the low spatial resolution due to the model size as well as lack of data with good quality, the model is able to represent only large-scale hydrogeological processes. Nevertheless, it reproduces the hydraulic head differences between main aquifer units as well as the significantly diverse flow directions within the different aquifer units. The transient model reproduces observed processes like the reversal of regional flow directions in north Jordan and the drying of two major springs or the ceasing of wadi baseflow. It also reflects the observed groundwater level decline as well as the vast heterogeneity of its temporal development throughout Jordan for different aquifers.

The fact that the model is able to represent the observed data at early times, but fails to reproduce the exacerbated decline at the end of the modelling period, especially in areas with intensive irrigated agriculture, is evidence that a significant amount of abstraction is unknown. An assessment

of the crop water demand based on satellite image evaluation revealed that groundwater abstraction for agriculture is about 75% higher than officially accounted. Using these higher abstraction rates, modelled heads fit better the observed groundwater levels. This clearly demonstrates that intensive groundwater abstraction for agricultural irrigation is the reason for the sudden increase in drawdown observed since 2010. The transient model depicts, thus, the illegal water abstraction for irrigation.

Scenario simulations until 2050 predict a continuous decline of groundwater levels and depicts areas with significant drawdown (up to 100 m). Partial reduction of groundwater abstraction considered under scenario 2 to comply with groundwater-by-law improves groundwater availability in the future, but does not fully reverse the adverse effects of recent developments.

These scenario results illustrate the consequences of current groundwater use and provide a basis for discussion among decision makers on future groundwater management. In addition, results show growing areas of aquifers that will become unsaturated in the future. This provides helpful information for future water allocations and the design of new wellfields.

A lack of available groundwater level data and insufficient monitoring of groundwater abstraction is a common phenomenon in many countries. This study shows the usefulness of applying remote sensing techniques to quantify agricultural water demand in order to fill these data gaps and thus improve groundwater modelling results.

Fig. 8 Simulated drawdown in A7/B2 from 2017 until 2050 for **a** scenario 1 and **b** scenario 2

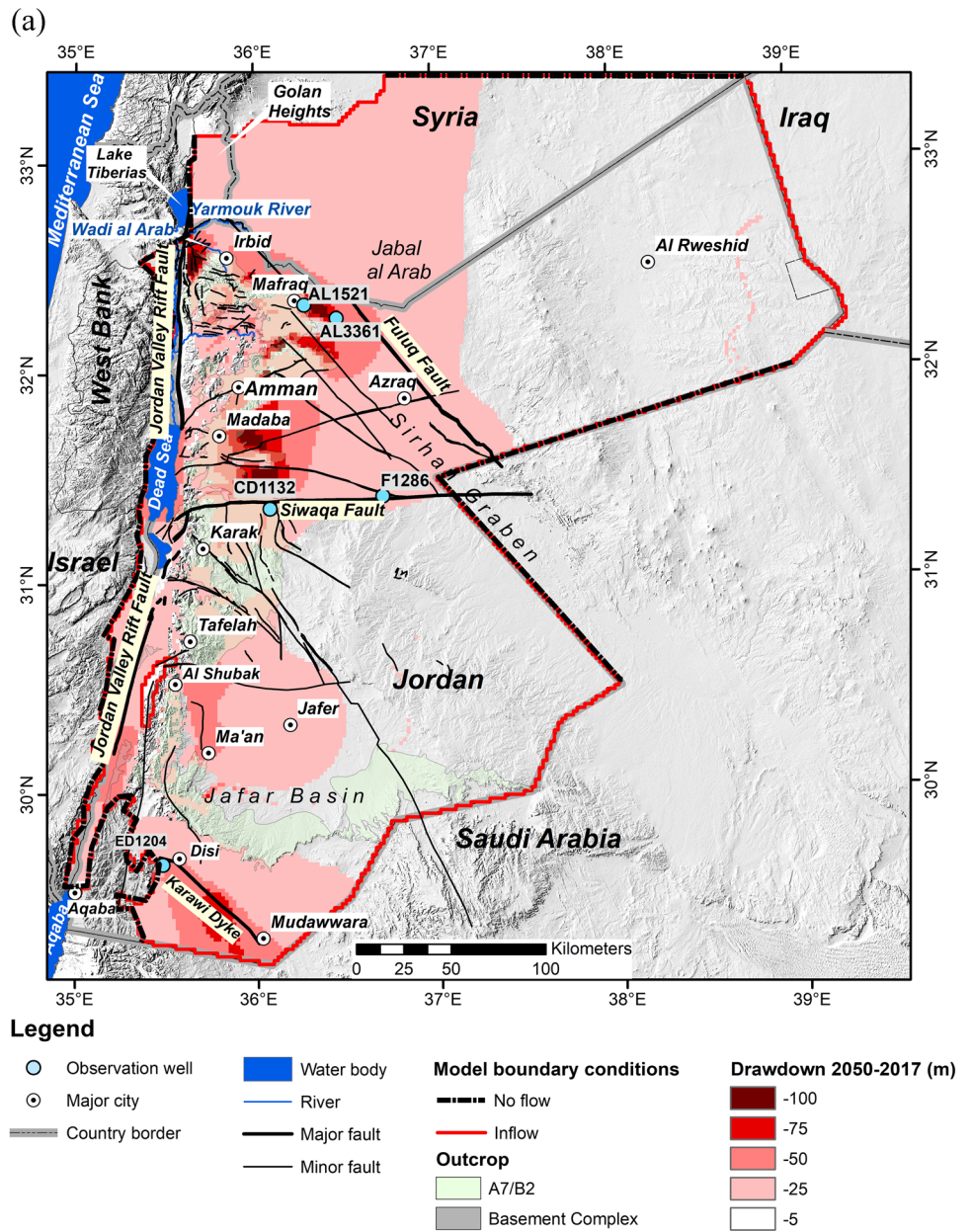
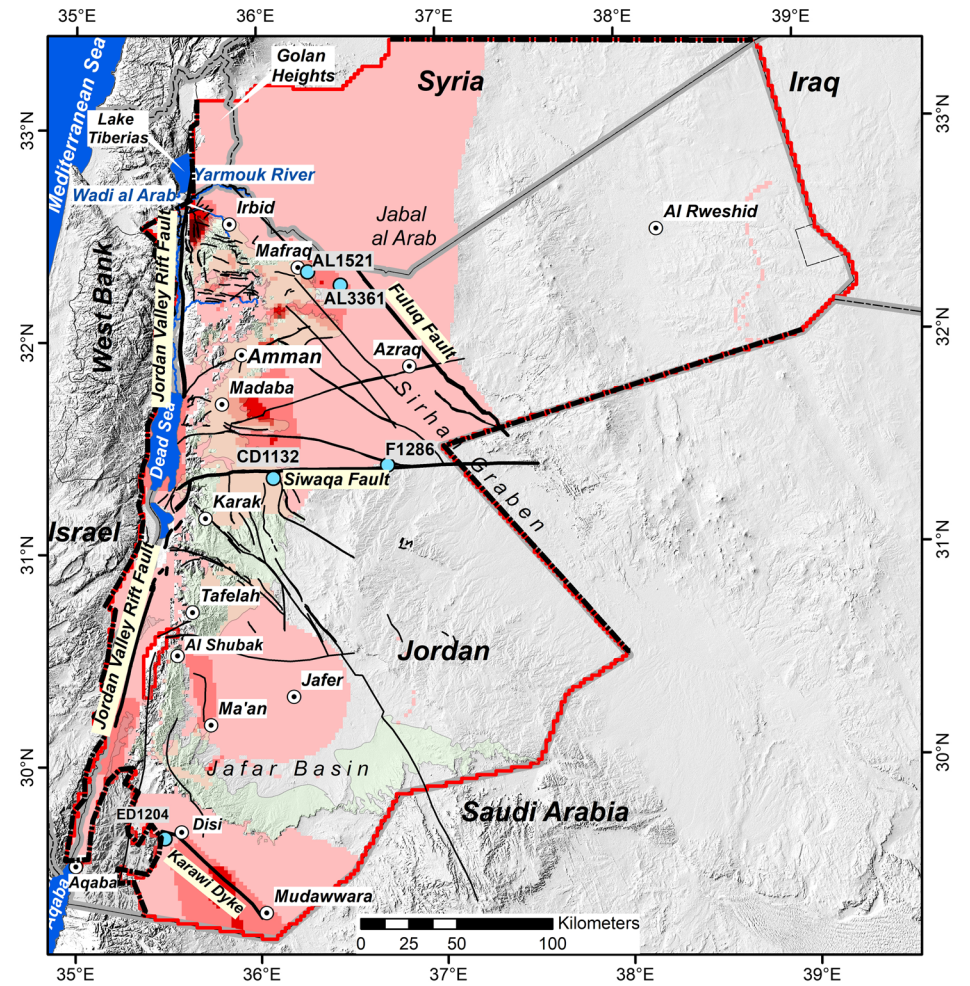


Fig. 8 (continued)

(b)



Legend

- | | | | |
|--------------------|---------------|----------------------------------|-------------------------------|
| ○ Observation well | ■ Water body | Model boundary conditions | Drawdown 2050-2017 (m) |
| ⊙ Major city | — River | --- No flow | ■ -100 |
| — Country border | — Major fault | — Inflow | ■ -75 |
| | — Minor fault | Outcrop | ■ -50 |
| | | ■ A7/B2 | ■ -25 |
| | | ■ Basement Complex | ■ -5 |

Funding Open Access funding enabled and organized by Projekt DEAL. This research was conducted within the framework of the technical cooperation project: “Management of Groundwater Resources” funded by the Federal Ministry for Economic Cooperation and Development (BMZ).

Declarations

Conflicts of interest On behalf of all authors, the corresponding author states that there is no conflict of interest.

Open Access This article is licensed under a Creative Commons Attribution 4.0 International License, which permits use, sharing, adaptation, distribution and reproduction in any medium or format, as long as you give appropriate credit to the original author(s) and the source, provide a link to the Creative Commons licence, and indicate if changes were made. The images or other third party material in this article are included in the article's Creative Commons licence, unless indicated otherwise in a credit line to the material. If material is not included in the article's Creative Commons licence and your intended use is not permitted by statutory regulation or exceeds the permitted use, you will need to obtain permission directly from the copyright holder. To view a copy of this licence, visit <http://creativecommons.org/licenses/by/4.0/>.

References

- Al-Bakri JT (2016) Mapping irrigated crops and estimation of crop water consumption in Amman-Zarqa Basin: a report for regional coordination on improved water resources management and capacity building. Ministry of Water and Irrigation, Amman, Jordan
- Allani M, Belhassen K, Huber M, Nouiri I, Tarhouni J (2019) Elaboration of a decision support system (DSS) for the Nebhana watershed, Tunisia, vol 1: regional cooperation in the water sector in the Maghreb. Technical report no. 2017.2213.1, Federal Ministry for Economic Cooperation and Development, Amman, Jordan
- Allen RG, Pereira LA, Raes D, Smith M (1998) Crop evapotranspiration. FAO Irrigation and Drainage paper 56, FAO, Rome, 293 pp
- Alsharhan AS, Rizk ZA, Nairn AEM, Bakhit DW, Alhajari SA (2001) Hydrogeology of an arid region: the Arabian gulf and adjoining areas. Elsevier, Amsterdam, 366 pp, eBook
- Armstrong HA, Abbott GD, Turner BR, Makhlof IM, Muhammad AB, Pedentchouk N, Peters H (2009) Black shale deposition in an upper Ordovician-Silurian permanently stratified, peri-glacial basin, southern Jordan. *Palaeogeogr Palaeoclimatol Palaeoecol* 273(3–4):368–377. <https://doi.org/10.1016/j.palaeo.2008.05.005>
- Bandel K, Salameh E (2013) Geologic development of Jordan: evolution of its rocks and life. Deposit no. 690/3/2013. <http://www.paleoiste.de/bandel/bandel2013.pdf>. Accessed July 2022
- Barthelemy Y, Béon O, le Nindre Y-M, Munaf S, Poittrinal D, Gutierrez A, Vandenbeusch M, Al Shoaibi A, Wijnen M (2007) Modelling of the Saq aquifer system (Saudi Arabia), chap 14. In: Chery L, de Marsily G (eds) Aquifer systems management: Darcy's legacy in a world of impending water shortage. Selected Papers on Hydrogeology 10, IAH, Wallingford, UK
- Barthelemy Y, Buscarlet E, Gomez E, Janjou D, Klinka T, Lasseur E, Le Nindre Y-M, Wuilleumier A (2010) Jordan deep aquifers modeling project. Final report. BRGM, Orleans, France
- Bender F (1974) Geology of Jordan. Borntäger, Berlin
- Bender F (1975) Geology of the Arabian Peninsula, Jordan, US Geol Surv Prof Pap 560-I
- Bender H, Hobler M, Klinge H, Schelkes K (1989) Investigations of groundwater resources in central Jordan. *Desalination* 72:161–170
- BGR/ESCWA (1996) Investigation of the regional basalt aquifer system in Jordan and the Syrian Arab Republic. 193 pp. <https://digitallibrary.un.org/record/242716>. Accessed 28 Jan 2022
- BGR/ESCWA (2013) Inventory of shared water resources in Western Asia. <http://waterinventory.org/sites/waterinventory.org/files/00-inventory-of-shared-water-resources-in-western-asia-web.pdf>. Accessed 28 Jan 2022
- Brückner F, Bahls R, Alqadi M, Lindenmaier F, Hamdan I, Alhiyari M, Atieh A (2021) Causes and consequences of long-term over-abstraction in Jordan. *Hydrogeol J*. <https://doi.org/10.1007/s10040-021-02404-1>
- Dodo A (2011) Iullemeden aquifer system: Mali - Niger – Nigeria, vol III. Sahara and Sahel Observatory, Tunis, Tunisia
- El-Naser H (1991) Groundwater resources of the deep aquifer system in NW Jordan: Hydrogeological and hydrogeochemical quasi 3-dimensional modelling. Forschungsergebnisse aus dem Bereich Hydrogeologie und Umwelt Angewandte Geologie und Hydrogeologie der Universität Würzburg, pp. 148
- FAO, UNDP (1968) Sandstone aquifers of East Jordan: report on computer procedures and programs for the analysis of project data. FAO, Rome and UNDP, New York
- FAO, UNDP (1972a) Development and use of groundwater resources of East Jordan: report on digital model of Qatrana wellfield area of East Jordan. FAO, Rome and UNDP, New York
- FAO, UNDP (1972b) Development and use of groundwater resources of East Jordan: report on digital model of Wadi Dhuleil area of East Jordan. FAO, Rome and UNDP, New York
- Gossel W, Ebraheem A, Wycisk P (2004) A very large scale GIS-based groundwater flow model for the Nubian sandstone aquifer in eastern Sahara (Egypt, northern Sudan and eastern Libya). *Hydrogeol J* 12:698–713
- Harbaugh AW (2005) MODFLOW-2005: the U.S. Geological Survey modular ground-water model—the ground-water flow process. US Geol Surv Tech Methods 6-A16. <https://doi.org/10.3133/tm6A16>
- Hijmans RJ, Cameron SE, Parra JL, Jones PG, Jarvis A (2005) Very high-resolution interpolated climate surfaces for global land areas. *Int J Climatol* 25:1965–1978. <https://doi.org/10.1002/joc.1276>
- Hobler M, Margane A, Almomani M, Subah A (1994) Groundwater resources of northern Jordan, vol 4: contributions to the hydrogeology of northern Jordan. Federal Institute for Geosciences and Natural Resources and Ministry of Water and Irrigation, Jordan
- Kalbus E, Oswald S, Wang W, Kolditz O, Engelhardt I, Al-Saud MI, Rausch R (2011) Large-scale modeling of the groundwater resources on the Arabian platform. *Int J Water Resour Arid Environ* 1(1):38–47
- Margane A, Saffarini I (1994) Groundwater resources of northern Jordan, vol 3: structural features of the main hydrogeological units in northern Jordan. Federal Institute for Geosciences and Natural Resources and Ministry of Water and Irrigation, Amman
- Margane A, Hobler M (1994) Groundwater resources of northern Jordan Vol. 3: structural features of the Main hydrogeological units in northern Jordan. Technical cooperation project “Advisory Services to the Water Authority of Jordan” BGR archive no. 118702:1-3, Federal Institute for Geosciences and Natural Resources, Amman
- Margane A, Zuhdi Z (1995) Groundwater resources of northern Jordan, vol. 1: rainfall, spring discharge and baseflow. Water Authority of Jordan and Federal Institute for Geosciences and Natural Resources, Amman

- Margane A, Almomany M (1995) Groundwater resources of northern Jordan, vol 2: groundwater abstraction – groundwater monitoring. Advisory Services to the Water Authority of Jordan in the field of hydrogeology. Federal Institute for Geosciences and Natural Resources, Amman
- Margane A, Hobler M, Almomani M, Subah A (2002) Contributions to the hydrogeology of northern and central Jordan. *Geologisches Jahrbuch Reihe C (Hydrogeologie, Ingenieurgeologie)*. Schweizerbart, Stuttgart, Germany
- Mull R, Holländer H (2006) Water supply of Tabuk and coastal towns and villages. Report on aspects of groundwater management with reference to the water resources of the transnational Saq aquifer in northern Saudi Arabia and southern Jordan. Institute of Water Resources Management, Hydrology and Agricultural Hydraulic Engineering, University of Hanover, Hanover, Germany
- MWI (2005) Nation water master plan 2005 digital version. Ministry of Water and Irrigation, Amman
- MWI (2018) Jordan water sector: facts and figures - 2017. Ministry of Water and Irrigation, Amman
- MWI, BGR (2019) Groundwater resources assessment of Jordan 2017. Amman, Jordan
- NASA (2020) Shuttle Radar Topography Mission data (SRTM). Earth elevation model available at: <https://www2.jpl.nasa.gov/srtm/>. Accessed July 2022
- Niswonger RG, Panday S, Ibaraki M (2011) MODFLOW-NWT, a Newton formulation for MODFLOW-2005, US Geol Surv Tech Methods 6-A37. <https://doi.org/10.3133/tm6A37>
- Nouiri I (2021) Elaboration of a decision support system (DSS) for the Nebhana watershed, Tunisia, vol 2. Regional cooperation in the water sector in the Maghreb. Technical report no. 2017.2213.1, Federal Ministry for Economic Cooperation and Development, Amman
- Powell JH (1989) Stratigraphy and sedimentation of the Phanerozoic rocks in central and South Jordan, part a: Ram and Khreim groups. Bull 11, Hashemite Kingdom Jordan Nat Resour Authority, Amman, 72 pp
- Powell JH, Abed AM, Le Nindre Y-M (2014) Cambrian stratigraphy of Jordan. *Georabia-Manama* 19(3):81–134. <http://nora.nerc.ac.uk/507989/1/PowellRamLV5Mar1.pdf>. Accessed 28 Jan 2022
- Salameh E (2008) Overexploitation of groundwater resources and their environmental and socio-economic implications: the case of Jordan. *Water Int* 33:55–68. <https://doi.org/10.1080/02508060801927663>
- Schmidt G, Subah A, Khalif N (2008) Model investigations on the groundwater system in Jordan: a contribution to the resources management (National Water Master Plan). In: Zereini F, Hötzl H (eds) *Climatic changes and water resources in the Middle East and North Africa*. Springer, Heidelberg, Germany, pp 347–359
- USGS - United States Geological Survey (1998) Overview of Middle East water resources. Water resources of Palestinian, Jordanian, and Israeli interest. Compiled for the Executive Action Team, Middle East Water Data Banks Project. <https://www.worldcat.org/title/overview-of-middle-east-water-resources-water-resources-of-palestinian-jordanian-and-israeli-interest-jordanian-ministry-of-water-and-irrigation-palestinian-water-authority-israeli-hydrological-service/oclc/234033584>. Accessed Jan 2022
- Wagner W (2011) *Groundwater in the Arab Middle East*. Springer, Germany, 443 pp
- Ziegler MA (2001) Late Permian to Holocene paleofacies evolution of the Arabian plate and its hydrocarbon occurrences. *GeoArabia* 6(3):445–504

Publisher's note Springer Nature remains neutral with regard to jurisdictional claims in published maps and institutional affiliations.